The foveal point spread function as a determinant for detail vision

Vision Research Vol. 21, pp. 1223 to 1233, 1981
Printed in Great Britain

0042-6989/81/081223-11$02.00/0
Pergamon Press Ltd

THE FOVEAL POINT SPREAD FUNCTION AS A DETERMINANT FOR DETAIL VISION

FRANS J. J. BLOMMAERT and JACQUES A. J. ROUFS
Institute for Perception Research, Den Dolech 2, P.O. Box 513, Eindhoven, The Netherlands

(*Received* 12 *February* 1981)

Abstract—A point spread function, chosen to link contrast sensitivity and stimulus dimensions, can be obtained from measured thresholds by assuming small-signal-linearity and peak detection for the visual system. To that end a special case of summation of subthreshold signals (perturbation) is used, taking specific measures against the effect of sensitivity drift. The basic assumptions are tested simultaneously and confirmed. Other provisional assumptions like radial symmetry and homogeneity were evaluated along a horizontal and a vertical meridian through the fovea. In the fovea no deviation from radial symmetry was found. The effect of inhomogeneity within the central fovea, seems to be too small to cause a significant change in the point spread function. The validity for predicting thresholds of stimuli exposing larger areas is tested. Annuli with varying radii show no significant aberration if probability summation is taken into account. Predicted disk thresholds, however, show a large discrepancy with experiment for radii larger than 2 min arc. A possible extension of the model with multiple-detection units having tuned sizes is evaluated.

INTRODUCTION

In order to investigate characteristics of detail vision stimuli like Landolt C's, lines or gratings are generally used. Sometimes, radially symmetrical stimuli like disks and annuli are used to investigate lateral processing over short distances (Fiorentini and Maffei, 1970; Westheimer, 1967). The spatial processing of the visual system is rather inhomogeneously over the retina. This is demonstrated by data on visual acuity (Le Grand, 1967) and thresholds for disks (Kishto, 1970; Wilson, 1970). A review is made by van Doorn *et al.* (1972). The effect is also found with thresholds of lines (Hines, 1976; Wilson and Bergen, 1979; Limb and Rubinstein, 1977). Wilson and Bergen, ibid, stressing the importance of local measurement of the inhomogeneous system, used line sources instead of gratings as stimuli. However, line sources of the usual type still stimulate retinal parts with different properties. The use of point sources is an obvious further step, the more so, since it is not clear how much the discrepancy between measured thresholds and prediction based on a line spread function (e.g. Wilson and Bergen, 1979) is disguised by effects of the mentioned extension of the lines.

A point spread or weighting function can be used to characterize the effect of a near-threshold-point-source on the contrast sensitivity of neighbouring retinal points (e.g. van Meeteren, 1973; Kelly, 1975). However, the threshold changes which have to be measured to obtain such a function are very small. Consequently special measures have to be taken to eliminate the effects of unavoidable sensitivity drift in order to obtain the required precision.

In this report the results of a technique to obtain a point spread function from threshold measurements is investigated and the predictive power is tested. This point spread function should represent the simple processing of the visual system, thus including optical effects. We started a first approximation of a model based on four plausible assumptions, namely quasi-linearity, local homogeneity, local radial symmetry and peak detection. On the basis of these assumptions, the spread of the activity of a point source is measured by using a special case of subthreshold summation of signals. The response of the test stimulus is kept so small that it perturbates the signal of the probing stimulus. This will be elaborated on, further on. A major effort was put in testing the basic assumptions.

Theoretical formalism

We assume that detection of quasi-static luminance increments can be formalized by using a peak detection model, i.e. a stimulus is seen if and only if the extreme value of the model's response $U(x, y)$ exceeds a certain level D. The threshold condition can then be written as

$$\text{extr}\{U(x, y)\} = D \qquad (1)$$

Furthermore we postulate that within a small area of the fovea the processing is:

homogeneous
radially symmetric
quasi-linear

The model is visualized in Fig. 1.

The response to an arbitrary small stimulus may, according to these assumptions, be written as a convolution integral with a local point spread function

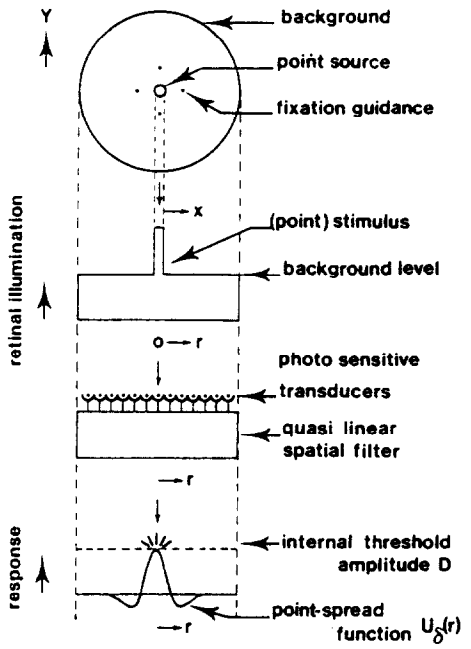

Fig. 1. Visualized detection model.

$U_\delta(x, y)$:

$$U(x, y) = \int_{-\infty}^{\infty} U_\delta(x - \bar{x}', y - y') \times \epsilon_f f(x', y')\, dx'\, dy' \quad (2)$$

Here $\epsilon_f f(x', y')$ is the distribution of retinal illumination of the stimulus ϵ_f being the amplitude parameter and $U(x, y)$ is the response of the visual system. From this equation it can be seen that, if the unit point spread function U_δ is known, the response to an arbitrary stimulus pattern can be calculated.

As we only deal with radially symmetrical stimuli in this paper, it is convenient to use polar coordinates, the response to the arbitrary stimulus becomes:

$$U(r) = \int_0^{2\pi} \int_0^{\infty} U_\delta(|r - r'|)\epsilon_f f(r') r'\, dr'\, d\psi' \times \underset{=}{\Delta} \epsilon_f U'(r) \quad (3)$$

In this equation, $U_\delta(r)$ is again the unit point spread function, which is radially symmetric according to the assumptions mentioned above; $U'(r)$ is the unit pattern response.

At threshold, the increment ϵ_f is given implicitly by incorporating this result in equation 1:

$$\epsilon_f \operatorname{extr}\{U'(r)\} = D \quad (4)$$

Perturbation approach

The unit point spread function can be determined by subthreshold summation. The response of a subthreshold pointstimulus can be probed by the response of another point on the basis of the assumptions mentioned above. By varying the intensity of the probe, the sum of the peak value of its response and the response of the teststimulus at a certain distance can be brought at threshold level. Since radial symmetry is assumed, the test stimulus at distance r can be replaced by a thin annulus with radius r in order to increase the effect.

If the response of the teststimulus is kept sufficiently small with respect to that of the probe, one might say that the response of the teststimulus perturbates that of the probe. This is highly analogous to the situation in the temporal domain explained in detail in Roufs and Blommaert (1981). The spatial case is worked out in the Appendix.

Apparatus and procedure

A four-way pseudo Maxwellian view optical system was used as is shown in Fig. 2. The subject viewed monocularly an 11° uniform field with a retinal illuminance of 1200 td. The stimuli used were superimposed on this field by using prisms. To facilitate fixation, four weak fixation lights with a radius of 2 min arc were projected around the stimulus on a circle with a dia of 1°. A 2 mm artificial pupil was used, which was provided with an entoptic guiding system to check the centering of the pupil of the eye (Roufs, 1963). The lights were generated by linearized glow modulators. The time functions used as an approximation of quasi-static presentation of the stimuli consisted of pulses of about 500 msec, the beginning

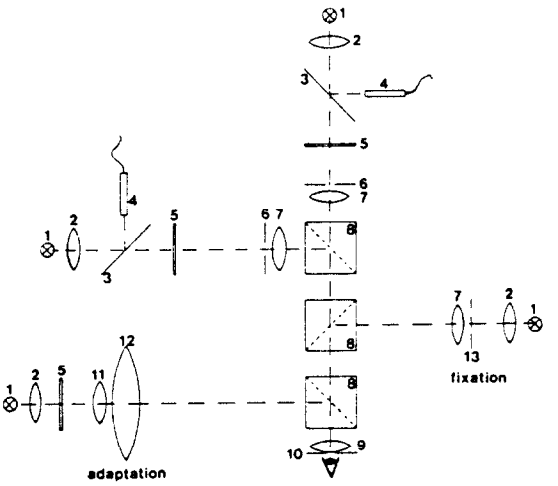

1 glow modulator
2 condensor
3 glass plate (mirror)
4 photodiode
5 neutral filter
6 stimulus
7 Maxwellian view lens
8 50% prism
9 ocular
10 2 mm artificial pupil
11 diverging lens
12 field lens
13 fixation marks

Fig. 2. Scheme of the optical apparatus.

and the end of which were smoothed in order to avoid transient phenomena. The luminance levels of the stimuli were kept in a constant ratio for reasons to be explained furtheron. The luminance levels were then simultaneously controlled by a dB step attenuator, after presetting the chosen ratio.

Via photodiodes, the luminance levels of the stimuli were recorded during the experiment, so that we were able to correct the results for minor luminance changes which occasionally occurred as a result of substantial temperature changes in the control circuitry.

The apparatus was checked for possible straylight artefacts by optical inspection of suitable stimuli using a microscope. No degeneration of any stimulus could be observed, so it was concluded that the optical spread of the apparatus was negligible compared with that of the optics of the human eye.

The subject had one knob to release the stimulus, which had to be detected. Three knobs enabled him to answer with "yes", "no" or "rejection". ("Rejection" is used if the subject feels he is deprived from the stimulus by lack of attention, blinking etc.).

All experimental data consisted of 50% luminance thresholds which were determined by the method of constant stimuli. At every intensity the detected fraction of 20 trials was determined. For one threshold, usually 3 to 4 different intensities were used, measured in random order for one psychometric function.

EXPERIMENTS

Experiment 1. Measuring a foveal point spread function

For this purpose we used a stimulus configuration as is shown in Fig. 3a. It consists of a small point-shaped stimulus (radius $r = 0.4$ min arc), surrounded by a concentric annulus of radius r_a and width Δr_a ($=0.4$ min arc). Both of these were superimposed on a constant background level of 1200 td.

In this experimental set-up, the retinal illumination of the annulus was chosen in such a way that it was always subthreshold (about 0.4 times its threshold value).

Furthermore it was kept in a constant ratio q to the retinal illumination of the point source, the technical realization of which was explained in the preceding section. In the experiment, we measured the threshold intensity of the point source in the presence of the perturbating annulus, compared with the threshold intensity of the point source without annulus.

It can be derived (see Appendix) from equation (3) that a discrete value for the point spread function (for one value of r, the radius of the annulus) can be calculated from the mentioned thresholds by:

$$U_\delta^*(r) = \frac{A_p}{qA_a}\left\{\frac{\epsilon_p}{\epsilon_{p,a}} - 1\right\} \tag{5}$$

$$\text{Norm factor} = \frac{U_\delta(o)}{D} = \frac{1}{\epsilon_p A_p} \tag{5b}$$

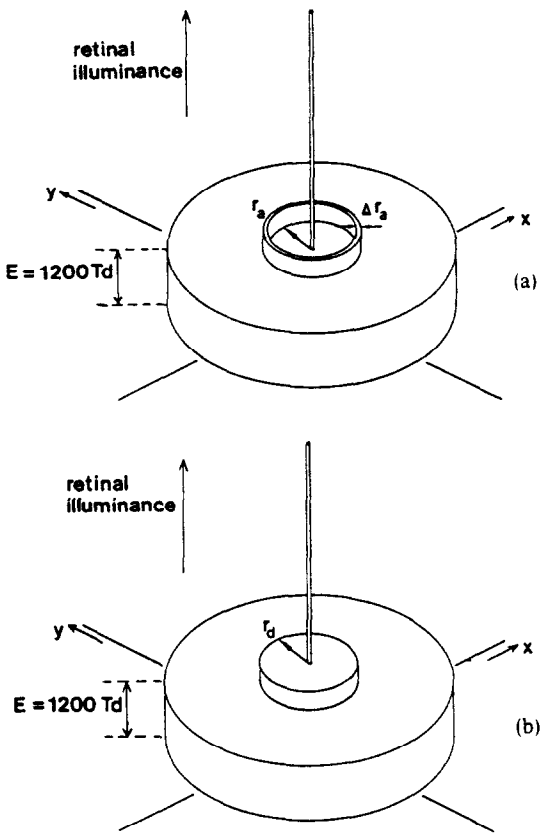

Fig. 3. Schematic drawings of the stimulus configurations used in (a) point spread function experiment and (b) test on linearity of processing.

Here,

$U_\delta^*(r)$ = the normalized unit point spread function,
A_p = area of the point,
A_a = area of the annulus,
ϵ_p = threshold intensity of the point alone,
$\epsilon_{p,a}$ = threshold intensity of the point surrounded by the annulus,
q = constant retinal illuminance ratio of annulus and point source
D = threshold level for the response.

By using a number of annuli with different radii r, a discrete number of values for the point spread function can be found.

To minimize the effect of sensitivity shifts of the subjects' system on the resulting value of U_δ^* according to equation (5) we took the following precautions:

—The paired thresholds ϵ_p and $\epsilon_{p,a}$ were always measured fast after one another (fast pair). The quotient $\epsilon_p/\epsilon_{p,a}$ is then almost independant of sensitivity shifts of the subject. (For further details on technique and statistical analysis see Roufs and Blommaert [1981]).

—Repetitions of all experimental sessions were carried out in a counterbalanced order, within the fast

pairs and within the complete experiment, to minimize the effect of systematic sensitivity changes, like fatigue.

Figure 4a shows the data of the normalized point spread function for one subject (F.B.). The absolute response, expressed in "D" units, can be found by multiplying the reduced values by the norm factor given in the legend.

This norm factor is found by averaging the threshold ϵ_p of the point alone over all 18 sessions necessary for the Experiments 1 and 2. In this way we tried to acquire an optimal representation of the average sensitivity of the subject. Per session, one point of the curve containing about 1100 trials, was measured, calculated from 8 fast pairs according to equation (5). The experimentally determined standard deviation of the mean is indicated. The order of measurement with respect to the r-axis was randomly chosen.

Experiment 2. Testing the linearity hypothesis

The stimulus configuration is shown in Fig. 3b and consists of a point-shaped stimulus superimposed on the centre of a subliminal disk on a 1200 td background level. The retinal illumination of the disk was again chosen in such a way, that it was always subthreshold, while it was kept in a constant ratio to the retinal illumination of the point source.

This configuration was chosen in order to imitate as closely as possible the experimental design of the first experiment. We argued that in trying to verify the linearity hypothesis, it would be better not to change the conditions with respect to the other basic assumptions.

Again we measured the threshold of a point source, the same percept to be detected as before. Instead of the ring a perturbating disk with variable diameter was used. Again the thresholds of the pointsource with and without perturbation were measured in fast pairs.

The result of the experiment can be interpreted (since the experiment is carried out for a number of disks with different radii) as a radially symmetrical negative-going edge spread function.

If this function is called $F(r)$, it can be calculated (see appendix) that:

$$F^*(r) = \frac{A_p}{q}\left\{\frac{\epsilon_p}{\epsilon_{p,d}} - 1\right\} \tag{6}$$

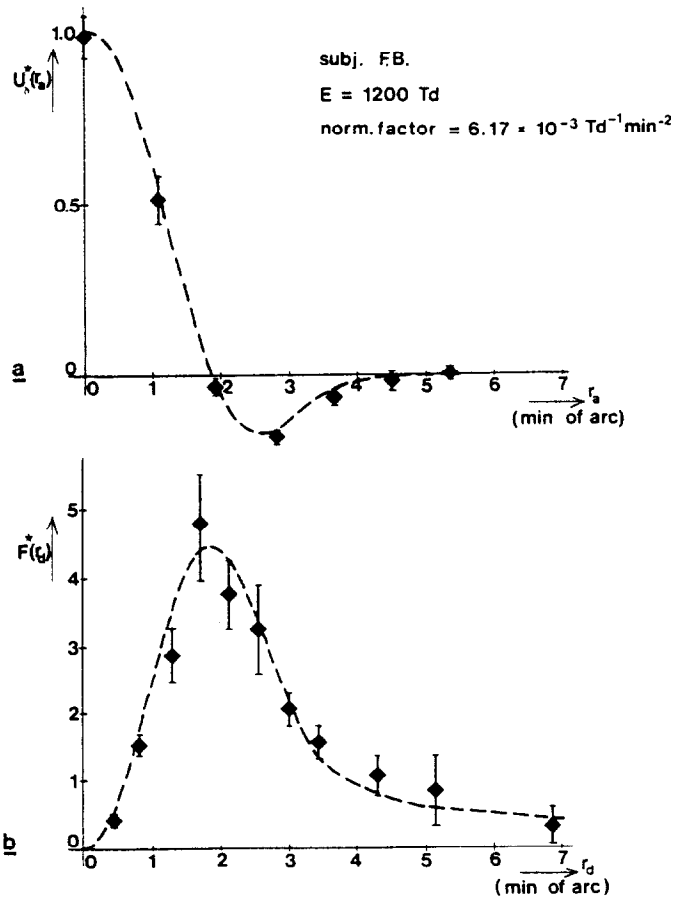

Fig. 4. Experimental data of (a) normalized point spread function $U_3^*(r)$ and (b) the response to a disk at its centre, with radius r_d of the disk as a parameter. The dashed curves are the results of a simultaneous computer fit. They exactly obey linearity of processing.

Here,

ϵ_p = threshold intensity of point alone,
$\epsilon_{p,d}$ = threshold intensity in the presence of the disk,
q = illuminance ratio of disk and point.

In experiment 2 we determined the response of a (negative going) radially symmetrical edge. If linearity is true there has to be a close relation with the response of the point-source of Experiment 1. For a linear space invariant system the derivative of a response to a unit edge equals the response to a unit point. The transformation to polar coordinates has to be taken into account. In the model this can be formalized by:

$$2\pi r U_s^*(r) = \frac{d}{dr} F^*(r) \qquad (7)$$

The results for the radially symmetrical edge spread function, according to equation (6), are shown in Fig. 4b. They were measured during 11 sessions, making an average of one point per session. All other conditions were the same as for the point spread function experiment. The dashed curves are the result of a simultaneous fitting to all data of both experiments in such a way that the relation of the two curves exactly obey equation (7). The curves were obtained by first multiplying the data of Fig. 4a by $2\pi r$. Since we experienced good results if the fitting was done in the frequency domain, the Fourier components of these results were averaged with those of dF^*/dr of Fig. 4b (differentiation was carried out in the frequency domain).

Finally, this average Fourier spectrum was transformed back to $U_s^*(r)$ and $F^*(r)$ respectively. As can be seen, both curves are highly consistent. This linearity test, which is commonly considered to be sensitive, appears to be positive.

Experiment 3. Testing homogeneity and global radial symmetry

For this purpose, the 50% thresholds of a point source (r = 0.4 min arc), were measured as a function of eccentricity over a horizontal and a vertical meridian through the fovea over a distance of about 3°.

In the case of homogeneity, all thresholds in whatever direction and at whichever eccentricity have to be the same. In the case of radial symmetry with respect to a certain point the variation of the threshold as a function of the distance to this point has to be independent of direction. Results with the fovea as a centre are shown in Fig. 5 (squares) on a semi-logarithmic scale. All points are the means of two thresholds. Of the four sessions, the first and second were used for measuring over the horizontal meridian while the third and fourth sessions were reserved for the vertical meridian. The order of measurement with respect to eccentricity was randomly chosen in the first and third sessions, while the order in the second was the reversed one of the first and the order of the fourth was reversed from the third.

In order to estimate the effect of short range inhomogeneity, the points up to 40′ were averaged over all four directions. With this range the change of threshold with distance can be described sufficiently accurate by a linear function as illustrated in Fig. 6a. The standard deviations of the means are also indicated. The straight line through the data points is the result of a regression computation, giving all data points the same weight. This finding was then incorporated in the model by assuming the retina to be linear-space-variant. The sensitivity was taken to vary with eccentricity according to the reciprocal of this threshold function. Since sofar we have no data of point spread functions at different eccentricities available, we were not able to take the change of the width of the point spread function into account. However, since the eccentricities used here are small, we do not anticipate this to be a considerable effect, estimating on the basis of the data of Hines (1976).

Experiment 4. Testing the threshold prediction of extended stimuli

To this end, we measured thresholds for annuli and disks with varying diameters and confronted these with the predicted thresholds from the model. An im-

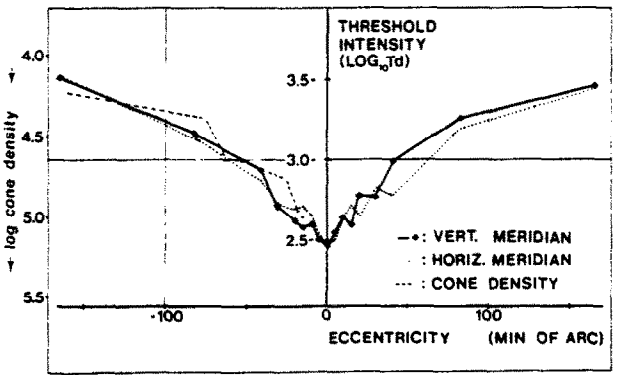

Fig. 5. Incremental thresholds of a point source along a horizontal and a vertical meridian through the fovea. For comparison, cone density in N/mm² (from Österberg, 1935) is plotted as open circles.

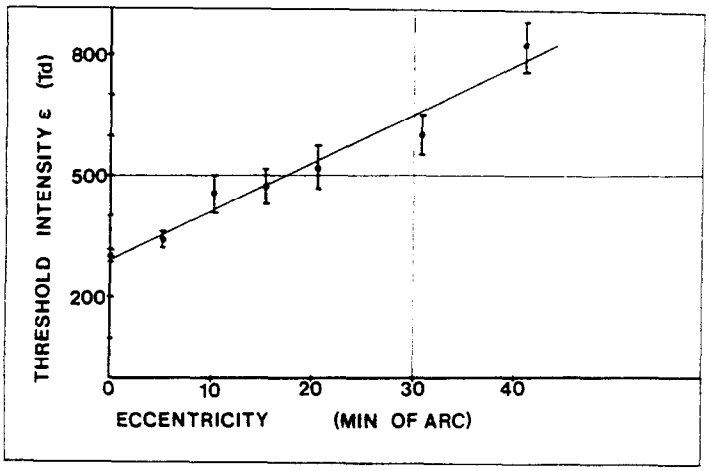

Fig. 6a. Averaged thresholds of a point source over four directions through the fovea. The straight line is a regression fit, giving all points the same weight.

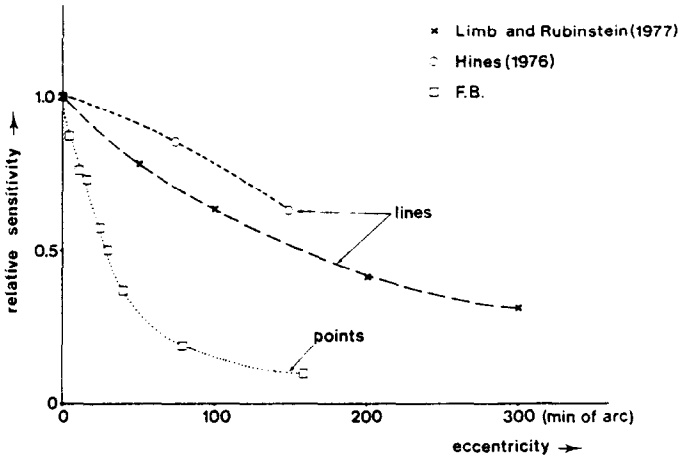

Fig. 6b. Sensitivity relative to the fovea for point and line stimuli. Sensitivity for points is derived from the thresholds as given in Fig. 5. Sensitivity for lines are taken from literature as shown in the legend.

portant difference with the foregoing experiments is that instead of a point larger areas have to be detected.

In Fig. 7 thresholds for annuli are plotted as a function of the mean radius. The experimental results are averages over two thresholds. The order of measurement with respect to the radius was randomly chosen in the first session and reversed in the second. The dashed line is the prediction according to equations (1) and (3).

The predicted values are in the right order of magnitude. For diameters larger than about 4 min arc, the measured values are about 0.3 log-unit below the predicted ones. However, this is not sufficient to violate the model since we have not yet taken into account the effect of stochastic fluctuations, which are responsible for the increase of detection probability if the stimulus area is enlarged.

Figure 8 shows a number of experimental results for disk thresholds as a function of the radius. All data points are averaged over two threshold values. By using reversed orders of measurement in different

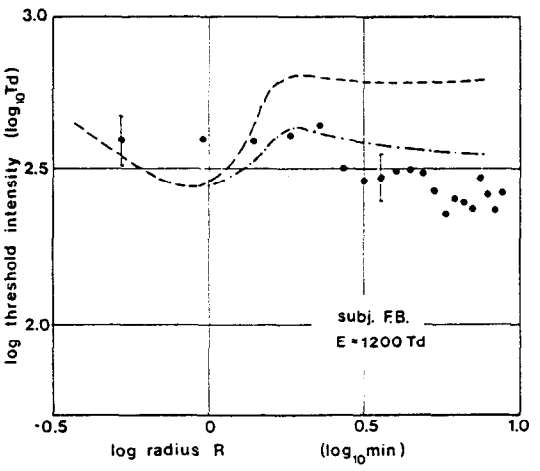

Fig. 7. Thresholds for annuli as a function of the mean radius. The dashed curve is the prediction of the model. The dotted line gives a correction for probability summation of the deterministic prediction. The distance between two horizontal bars covers the average difference of two thresholds of which the means are indicated by the dots.

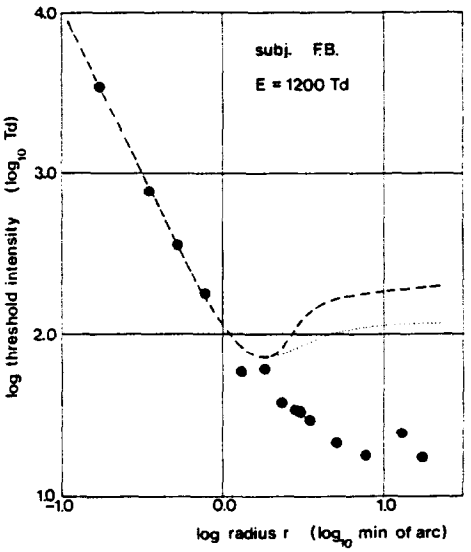

Fig. 8. 50% thresholds for incremental foveal disks as a function of the radius. The dashed curve is the deterministic prediction from the model. The dotted line is a correction for probability summation.

sessions, counterbalancing was again used as a tool to minimize the effect of systematic sensitivity drift on the final result. The dashed line is again the prediction from the model.

Keeping in mind that there is no free parameter, the prediction for small diameters is very good. However, for diameters larger than about 4 min arc, there is a distinct deviation between prediction and experiment. This will be discussed in greater detail further on.

* Note added in revised text: after submission of this paper Barbur and Ruddock (1980) published point spread functions obtained with targets moving across spatially structured background fields. Their data are quite close to ours.

DISCUSSION

As one can clearly see from Fig. 4, the responses measured with perturbation approach are fairly large in comparison with the spread.

The measured point spread function of our subject, has about the same shape as Fiorentini and Maffei's (1970) based on the effect of steady annuli with variable diameters on the incremental threshold of a small disc (dia 1.7 min arc). They also concluded for an excitatory centre surrounded by an inhibitory region. However, the spatial extension of our point spread function is somewhat less (width of centre of about 4 min arc against 7 min arc for Fiorentini and Maffei), which is probably due to our adaption level of 1200 td against 100 td in their experiments*. A difference of about a factor 2 due to these different adaptation levels, is to be expected on the basis of visual acuity data as a function of adaptation level (see for instance Nakane and Ito, 1978).

It is of some interest to compare the present point spread function with line spread functions from literature assuming an infinite length, linearity and homogeneity. Using Hankel and Fourier algorithms, transformed data of Hines, 1976; Kulikowski and King-Smith, 1973; Limb and Rubinstein, 1977 are drawn in Fig. 9. Although one has to take into account the effect of inhomogeneity, different line lengths and background levels used, the differences in the obtained point spread functions suggest that this kind of transformation is too simple to obtain a satisfactory point spread function.

According to Fiorentini *et al.* (1972), who found no summation if a disk is presented to one eye and an annulus to the other, the described interaction between signals of different retinal elements has to take place at a location before binocular convergence of signals occurs.

Furthermore, it is noteworthy that the width of the excitatory centre at this relatively high background level is not much larger than the optical spread given

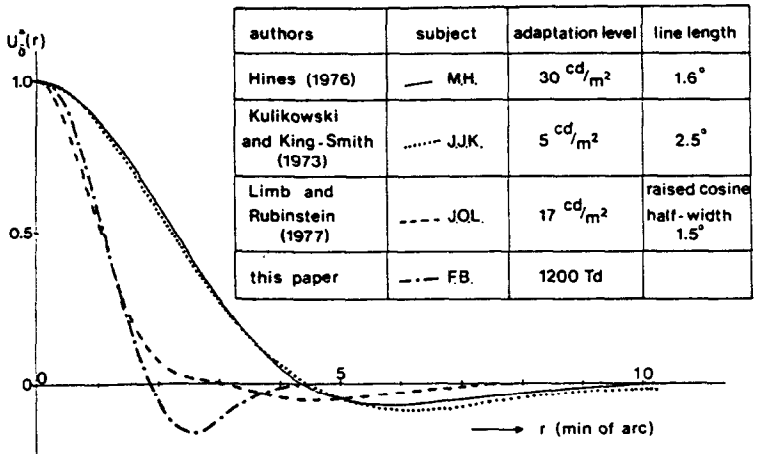

authors	subject	adaptation level	line length
Hines (1976)	—— M.H.	30 cd/m²	1.6°
Kulikowski and King-Smith (1973)	..... J.J.K.	5 cd/m²	2.5°
Limb and Rubinstein (1977)	- - - - J.O.L.	17 cd/m²	raised cosine half-width 1.5°
this paper	—·— F.B.	1200 Td	

Fig. 9. Normalized point spread functions derived from line spread functions measured by different authors and calculated on the basis of assumptions, mentioned in the text. For comparison the measured point spread function of Fig. 4 is shown.

by Vos *et al.* (1976) for human eyes with pupil dia of 2 mm. This could mean that from the excitatory lateral processing in the fovea, the spread of the optical system is at least an important part. This probably is not the case at low levels of adaptation or in the periphery, as will be shown in a subsequent paper.

Figure 4 shows that, within measuring precision, all experimental points lie on the dashed curves, which obey the basic linearity and peak detection postulates exactly. Linear lateral processing seems to be a good approximation in this case.

Looking at the three-dimensional plots of point- and disk-responses computed from the model, as shown in Fig. 10, it can be appreciated why $F^*(r)$ of Fig. 4b becomes zero for large values of r: For small disk radii the core of the point spread function determines the integrating effect; for large radii the inhibiting part gradually diminishes the effect.

From Fig. 5, which shows the results for thresholds of a point source as a function of eccentricity, it can be seen that there is no significant difference between the results on the vertical and the horizontal meridian. Since we did not measure in oblique directions, aberrations from radial symmetry of this eccentricity effect cannot be excluded. The magnitude of the threshold variations are compatible with findings of Kishto (1970) and of Wilson (1970), who measured with disks.

Note from Fig. 5 that the effect follows very closely the density of cones as a function of eccentricity as reported by Österberg (1935), although the connection is not obvious since other mechanisms take part. Compared with the effect of eccentricity on sensitivity as measured with lines (Hines, 1976; Wilson and Bergen, 1979 and Limb and Rubinstein, 1977), ours is more pronounced (Fig. 6b). One reason is probably that the spatial extension of lines flattens out the actual retinal inhomogeneity. Another is that our background luminance is higher.

One aspect of the measurement should not be left unmentioned, i.e. the possible effect of involuntary eye movements on the results of the experiments. As can be seen from Fig. 5, the fovea itself looks like some sort of singular point. Because of eye movements, the real singularity may very well be flattened out by the averaging effect that involuntary eye movements have. According to Ditchburn (1973), the magnitude of the eye movements in a situation where good fixation is maintained, can be described roughly by a normal distribution with a σ-value of 2 to 3 min arc. This would apply to our conditions (self release by subject after fixation; fixation periods of less than a second) and indicates a possible smoothing of the real inhomogeneity as a result from averaging within a gaussian window of 2–3 min arc.

Concerning the perturbation experiments, it should be kept in mind that small saccades are not likely to interfere much with the results of the experiment because the relative position of point- and perturbation-stimulus is not affected by eye movements.

The data of Fig. 5 were averaged over all four directions and replotted for a limited range in Fig. 6a.

The increase of threshold as a function of eccentricity can be well approximated by a straight line over a distance of 40 min arc from the fovea. Taking the effect of inhomogeneity into account, the original model was transformed to a spatial variant one in such a way, that the norm factor of the point spread function decreases with the distance to the fovea as the reciprocal of the values prescribed by the straight line of Fig. 6a.

It turned out that in view of the distances involved the corrections to be applied to the point and edge spread function were small with respect to the experimental error.

In Fig. 7, the experimental thresholds for annuli are compared with the prediction of the model. Taking into account the effect of daily sensitivity variations, the prediction of thresholds of annuli with small radii is not bad. For radii larger than about 2 min arc there seems to be some discrepancy. However, this can be explained by threshold decrease caused by the increase of probability of detection of larger areas, the so called probability summation.

A rough estimation of the effect was carried out by treating the problem as a discrete one. It was assumed that foveal areas of 1 min^2 had an independent chance of reaching a stochastic threshold value. On the basis of this, it was calculated how many independent areas annulus responses had in comparison to a point response (which, by definition, consisted of one area). By using stochastic calculations based on the slope of the measured psychometric functions (cf. Roufs, 1974) the effect of increased probability on the 50% threshold was then calculated and the corrected values are shown as dotted lines in Fig. 7. It was found from calculations based on integration areas of 0.5 and 2 min^2, not shown here, that for the present stimulus dimensions the effect does not depend heavily on the knowledge of the exact integration area.

For disks, Fig. 8 gives the experimental thresholds, together with prediction. Now, for radii larger than 2 min arc, a substantial difference is observed between prediction and experiment, which increases as the diameter of the disk increases. A similar discrepancy between model and experiment is reported by investigators who work with line spread functions: if thresholds for bars are compared with theoretical thresholds from a single-unit model, the experimental thresholds are usually lower than the predicted ones (Kulikowsky and King-Smith, 1973; Hines, 1976). There just seems to be more integration by the visual system than is expected on the basis of point or line spread functions. With lines the results may be distorted by the effect of their extension over a relatively large part of the inhomogeneous retina. Using a point spread function, which would provide a clearer picture in that aspect the discrepancies found (for disks) are even larger.

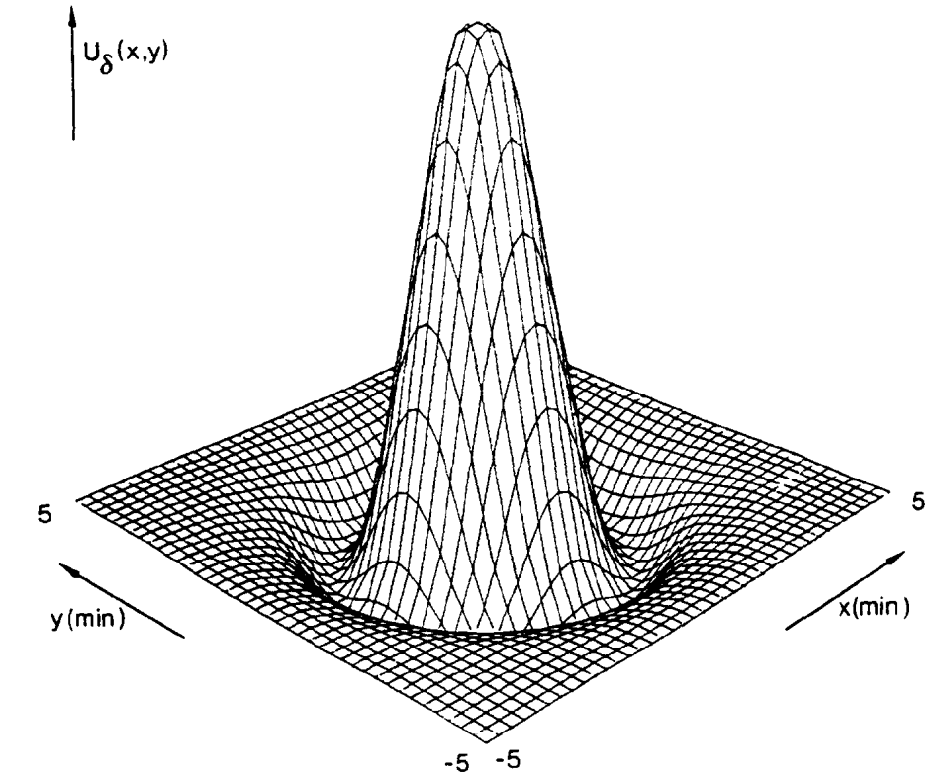

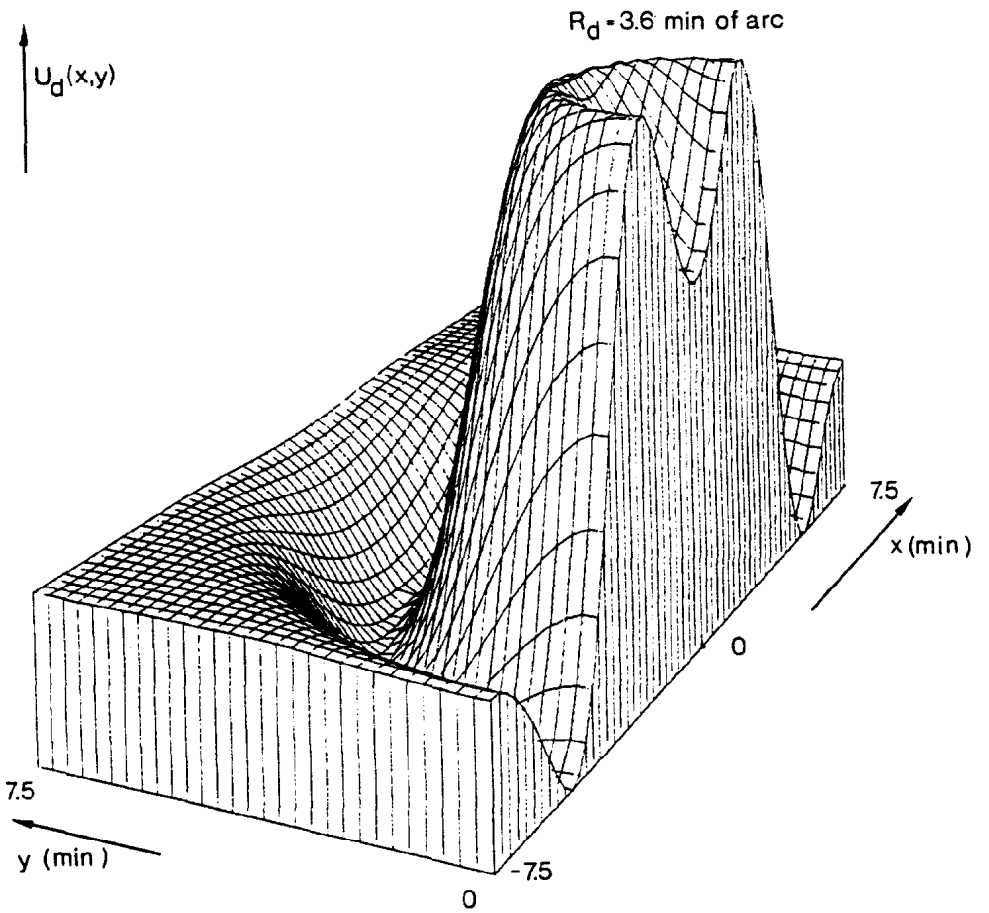

Fig. 10. Top: three-dimensional plot of the point spread function of Fig. 4a. Bottom: intersection of 3D plot of calculated response of the model on a disk with radius r_d = 3.6 min arc.

One approach to deal with this partial disaccordance has been provided by among others: Sperling (1970), Thomas (1970), Koenderink and van Doorn (1978) and Wilson and Bergen (1979). These authors have propositions for the visual system in common, which consist of an ensemble of units (receptive fields or line spread functions) working at one spatial coordinate of the retina and that vary in extension and sensitivity. Bagrash's (1973) psychophysical evidence for size-tuning seems to support this idea. The most detailed model is worked out by Wilson and Bergen (1979) which has four line spread mechanisms working at each retinal eccentricity that differ in width and sensitivity and contains probability summation, which is formalized in an algorithm put forward by Quick (1974).

Exploring the potentialities of such a multiple unit model we assumed 4 isomorphic point spread mechanisms, the narrowest being equal to the measured one. The width of every next mechanism is increased by a factor 2 and the amplitude is fitted to the disk threshold data as shown in Fig. 11. Such an extension of the model is apparently able to account for the disk data. If the mechanisms are independent or weakly dependent like in the Wilson and Bergen model this does not alter the point and the edge spread functions nor does it change the prediction of the thresholds of annuli. (A test in relation with other stimulus shapes will be reported in a subsequent paper).

In view of the scatter in receptive field sizes found electrophysiologically in the retina (Fischer, 1973) and in the striate cortex (Hubel and Wiesel, 1974) a four mechanisms model seems rather artificially. On the other hand it might be a way to approximate a more natural but also more difficult to handle model as the one proposed by Koenderink and van Doorn (1978), having a continuous receptive field size distribution.

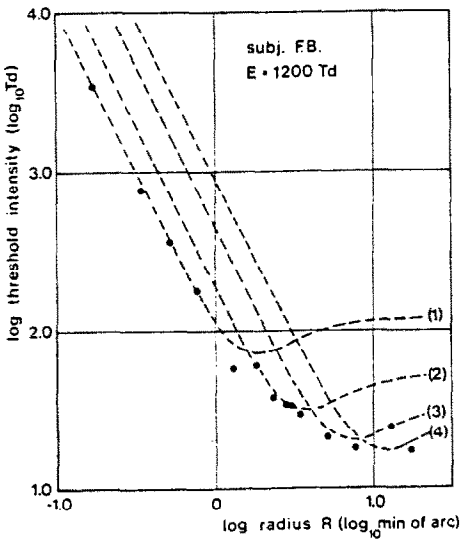

Fig. 11. Illustration of fitting a "four-mechanism model" to disk thresholds as a function of the radius. The smallest mechanism (1) is described completely by the measured point spread function, probability summation included. Mechanisms (2), (3) and (4) have the same shape but increase in width with a factor 2. The dashed curves are the predictions from the individual mechanisms.

CONCLUSIONS

Point and edge spread functions determined by using a point source as a probe are quantitatively mutually consistent.

If the point spread function is used to predict thresholds of larger stimuli the effect of increased detection probability extending the stimulus area does effect a non neglectable threshold decrease.

Quantitative correction based on independent area elements seems to be adequate for slim stimuli. However, "probability" summation cannot explain the threshold lowering for more "square" stimuli.

A multi-mechanism model, including probability summation can account for our results but is not necessarily the best one.

Acknowledgement—The authors are indebted to the Netherlands Organization for the Advancement of Pure Research (Z.W.O.) for providing financial support for this investigation.

REFERENCES

Bagrash F. M. (1973) Size-selective adaptation: psychophysical evidence for size-tuning and the effects of stimulus contour and adapting flux. *Vision Res.* **13**, 575–598.

Barbur J. L. and Ruddock K. H. (1980) Spatial characteristics of movement detection mechanisms. Human Vision-I Achromatic vision. Biol. Cybernet. **37**, 77–92.

Blommaert F. J. J. (1977) Spatial processing of small visual stimuli. *IPO A. Prog. Rep.* **12**, 81–86.

Ditchburn R. W. (1973) *Eye-Movements and Visual Perception*. Clarendon Press, Oxford.

Doorn A. J. van, Koenderink J. J. and Bouman M. A. (1972) The influence of the retinal inhomogeneity on the perception of spatial patterns. *Kybernetik* **10**, 223–230.

Fiorentini A. and Maffei L. (1970) Transfer characteristics of excitation and inhibition in the human visual system. *J. Neurophysiol.* **33**, 285–292.

Fiorentini A., Bayly E. J. and Maffei L. (1972) Peripheral and central contributions to psychophysical spatial interactions. *Vision Res.* **12**, 253–259.

Fiorentini A. (1977) Centre-surround concepts, luminance gradients and contrast. In *Spatial Contrast, Report of a Workshop* (Edited by Spekreijse H. and Tweel L. H. van der), pp. 38–40. North Holland, Amsterdam.

Fischer B. (1973) Overlap of receptive field centers and representation of the visual field in the cat's optic tract. *Vision Res.* **13**, 2113–2120.

Hines M. (1976) Line spread function variation near the fovea. *Vision Res.* **16**, 567–572.

Hubel D. H. and Wiesel T. N. (1974) Uniformity of monkey striate cortex: a parallel relationship between field size, scatter, and magnification factor. *J. comp. Neurol.* **158**, 295–306.

Kelly D. H. (1975) Spatial frequency selectivity in the retina. *Vision Res.* **15**, 665–672.

Kishto B. W. (1970) Variation of the visual threshold with retinal location. *Vision Res.* **10**, 745–767.

Koenderink J. J. and Doorn A. J. van (1978) Visual Detection of spatial contrast: influence of location in the visual field, target extent and illuminance level. *Biol. Cybernet.* **30**, 157–167.

Kulikowski J. J. and King-Smith P. E. (1973) Spatial arrangement of line, edge and grating detectors revealed by subthreshold summation. *Vision Res.* **13**, 1455–1478.
Meeteren A. van (1973) Visual aspects of image intensification. Thesis Utrecht.
Le Grand Y. (1967) *Form and Space Vision*. Indiana Univ. Press, Bloomington.
Limb J. O. and Rubinstein C. B. (1977) A model of threshold vision incorporating inhomogeneity of the visual field. *Vision Res.* **17**, 571–584.
Nakane Y. and Ito K. (1978) Study on standard visual acuity curves for better seeing in lighting design. *J. Light Vis. Env.* **4**, 38–44.
Österberg G. (1935) *Topography of the Layer of Rods and Cones in the Human Retina*. Arnold Busch, Copenhagen.
Quick R. F. (1974) A vector-magnitude model of contrast detection. *Kybernetik* **16**, 65–67.
Rodieck R. W. and Stone J. (1965) Analysis of receptive fields of cat retinal ganglion cells. *J. Neurophysiol.* **28**, 833–849.
Roufs J. A. J. (1963) Perception lag as a function of stimulus luminance. *Vision Res.* **3**, 81–91.
Roufs J. A. J. (1974) Dynamic properties of vision VI Stochastic threshold fluctuations and their effect on flash-to-flicker sensitivity ratio. *Vision Res.* **14**, 871–888.
Roufs J. A. J. and Blommaert F. J. J. (1975) Pulse and step response of the visual system. *IPO A. Prog. Rep.* **10**, 60–67.
Roufs J. A. J. and Blommaert F. J. J. (1981) Temporal impulse and step responses of the human eye obtained psychophysically by means of a drift-correcting perturbation technique. *Vision Res.* **21**, 000–000.
Sperling G. (1970) Model of visual adaptation and contrast detection. *Percept. Psychophys.* **8**, 143–157.
Thomas J. P. (1970) Model of the function of receptive fields in human vision. *Psychol. Rev.* **77**, 121–134.
Thomas J. P. (1978) Spatial summation in the fovea: asymmetrical effects of longer and shorter dimensions. *Vision Res.* **18**, 1023–1029.
Vos J. J., Walraven J. and Meeteren A. van (1976) Light profiles of the foveal image of a point source. *Vision Res.* **16**, 215–219.
Westheimer G. (1967) Spatial interaction in human cone vision. *J. Physiol.* **190**, 139–154.
Wilson H. R. and Bergen J. R. (1979) A four mechanism model for threshold spatial vision. *Vision Res.* **19**, 19–32.
Wilson M. E. (1970) Invariant features of spatial summation with changing locus in the visual field. *J. Physiol.* **207**, 611–612.

APPENDIX

For a small stimulus, approximating a point source with retinal illuminance ϵ_p and radius r_o, the response pattern of the visual system can, according to equation 3, be written as

$$U_p(r) = \epsilon_p \int_0^{2\pi} \int_0^{r_0} r' U_\delta(|r - r'|)\, dr'\, d\psi'.$$

Due to the basic assumptions for determining threshold and assuming that the point is situated foveally, only the response for $r = 0$ is of interest, so

$$U_p(0) = \epsilon_p \int_0^{2\pi} \int_0^{r_0} r' U_\delta(r')\, dr'\, d\psi'.$$

If r_0 is taken sufficiently small, this can be approximated by

$$U_p(0) \approx \epsilon_p A_p U_\delta(0),$$

where A_p is the area of the point.

The threshold condition of a point may now be formalized as

$$\epsilon_p A_p U_\delta(0) = D \tag{8}$$

If perturbation of a point response is applied with an arbitrary shape, equation (8) changes into

$$\epsilon_{p,pert} A_p U_\delta(0) + U_{pert}(0) = D \tag{9}$$

Here $U_{pert}(0)$ is the response in the origin of the perturbating stimulus. $\epsilon_{p,pert}$ is the retinal illumination of the point source necessary for detection of the combination.

Of course, equation (9) is valid only if the retinal illuminance of the perturbation is so small that detection is always governed by the extremum of the point response. Since D is in fact a stochastic magnitude, the intensity of the test stimulus should also be kept small in order to avoid a substantial contribution of its response to the detection chance.

In the first experiment we used an annulus with mean radius r_a and width Δr_a. It can easily be verified from equation (3) that for $\Delta r_a \ll r_0$ its response in the origin can be approximated by

$$U_a(0) = \epsilon_a 2\pi r_a \Delta r_a U_\delta(r_a) = \epsilon_a A_a U_\delta(r_a).$$

If $\epsilon_a/\epsilon_{p,a} = q$, where $\epsilon_{p,a}$ is the threshold of the point-annulus configuration, we can write for the threshold condition of this combination

$$\epsilon_{p,a}\{A_p U_\delta(0) + qA_a U_\delta(r_a)\} = D.$$

As pointed out above, q should be small. Comparing the threshold with and without annulus $\epsilon_{p,a}$ and ϵ_p we are able to derive for the normalized point spread function $U^*_\delta(r_a)$

$$U^*_\delta(r_a) = \frac{U_\delta(r_a)}{U_\delta(0)} = \frac{A_p}{qA_a}\left\{\frac{\epsilon_p}{\epsilon_{p,a}} - 1\right\}.$$

We can again find the absolute response by multiplying U^*_δ with its absolute value $U_\delta(0)$ expressed in "D" units, which can be computed from equation 5b.

In the second experiment we used a disk with radius r_d as perturbation.

It can be seen from equation (3) that for the response pattern of a uniform disk at $r = 0$ we can write (subscript "d" for disk)

$$U_d(0) = 2\pi\epsilon_d \int_0^{r_d} r U_\delta(r)\, dr.$$

If $\epsilon_d/\epsilon_{p,d} = q$, this leads to the threshold condition

$$\epsilon_{p,d}\left\{A_p U_\delta(0) + 2\pi q \int_0^{r_d} r U_\delta(r)\, dr\right\} = D.$$

From the threshold change we can derive for the response $F^*(r_d)$ on a negative-going radial symmetrical edge.

$$F^*(r_d) = 2\pi \int_0^{r_d} r U^*_\delta(r)\, dr = \frac{A_p}{q}\left\{\frac{\epsilon_p}{\epsilon_{p,d}} - 1\right\} \tag{10}$$

By using disks with different radii r_d, we will find a discrete number of samples for $F^*(r_d)$, which has a unique relationship with the normalized point spread function $U^*_\delta(r)$ as is expressed in equation (7).